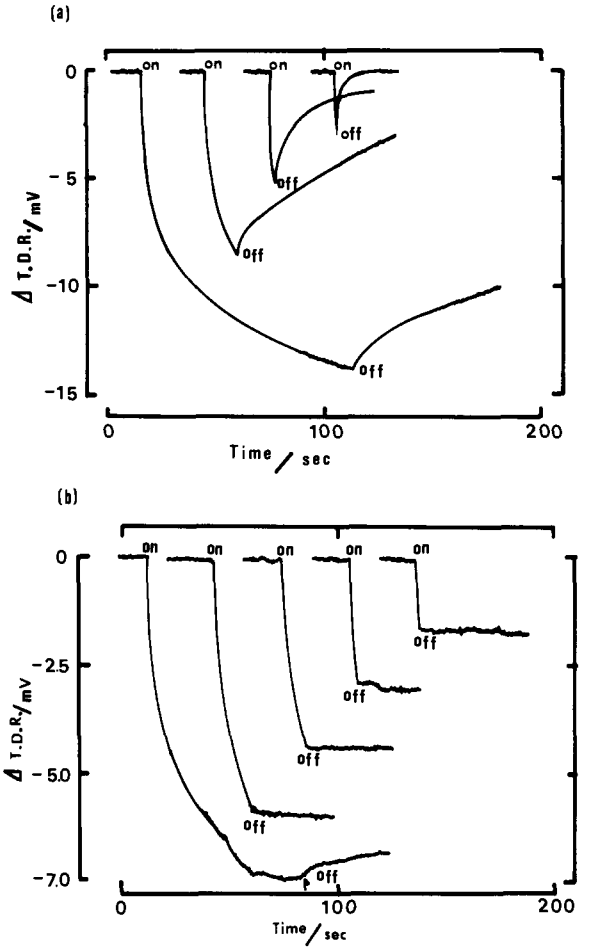

Figure 2. Time-dependent profile of the TDR signal; "on" and "off" in the figures show the starting and end point of the irradiation, respectively. MV^{2+} was added in (a); no MV^{2+} was added in (b).

Typical results are shown in Figure 2a,b which correspond to two cases: when an electron acceptor (10^{-3} M MV^{2+}) was added to the alcohol and when no electron acceptor was added, respectively. In both cases, the photoexcited reaction caused the TDR signal to be shifted -10 mV from its initial value. However, at the end of the photoexcitation, the behavior of the TDR signals was totally different for the suspensions with and without the electron acceptor. For example, in the case for which the acceptor was present, the TDR signal returned to the initial level (Figure 2a) and the time constants of the growth depended on the total time of irradiation. However, when an electron acceptor was absent a growth of the TDR signal was not observed (Figure 2b).

These results are explained as follows. The photocatalytic reaction that occurs in the TiO_2 suspension causes changes in electrical properties of the suspension, i.e., the impedance of the BDCE, and then this change is detected by the TDR signal. The electrical properties of the suspension may be determined by several factors including (1) the concentration and mobility of the free carriers in the TiO_2 particles, (2) the distribution and concentration of ions around the particles, and (3) the conformation of the solvent dipoles at the particle surface. Initially, electron-hole pairs are created in the TiO_2 particles by the photoexcitation, and the concentration of the free carriers in the TiO_2 is increased. The changes in the free carrier concentration in the semiconductor particle will affect the surface potential of the particle and then the distribution of ions around the particle, which causes the change in the dielectric property of the suspension.[5,6] However, the concentration of the ions in the suspension is approximately constant because the nonreactive electrolyte (Na_2SO_4) is present. The change in the surface potential will also affect the conformation of the dipoles of the solvent molecules. Therefore, the impedance of BDCE and the TDR signal are controlled mainly by the concentration of the carriers in the particles.

Holes created by the photoexcitation are transferred to the solvent ethanol, and then the electrons accumulate in the particle, if an electron acceptor is not present in the suspension. When an electron acceptor MV^{2+} is present, the electron accumulation will be decreased, but the accumulation can still occur if the hole-transfer rate is faster than the electron-transfer rate to the electron acceptor. After the cessation of the irradiation, the discharge of the accumulated electrons in the particle is more rapid if MV^{2+} is present. The rate of discharge is controlled by the diffusion of MV^{2+} in the ethanol to the surface of the particles. Then, the rate of discharge is slower for long-term than short-term irradiation because the length of the diffusion layer of MV^{2+} is increasing (i.e., the concentration gradient of MV^{2+} is decreasing) as the photocatalytic reaction proceeds. From this explanation, it is the accumulated electrons in the TiO_2 particle that shift the TDR signal.

To our knowledge, this is the first experiment in which TDR has been applied to study photochemical reactions, especially photocatalytic reactions occurring on semiconductor particles.

Registry No. TiO_2, 13463-67-7; MV^{2+}, 4685-14-7; ethanol, 64-17-5.

(5) Schwan, H. P.; Schwarz, G.; Maczuk, J.; Pauly, H. *J. Phys. Chem.* **1962**, *66*, 2626.

(6) (a) Chew, W. C.; Sen, P. N. *J. Chem. Phys.* **1982**, *77*, 4683. (b) Chew, W. C.; Sen, P. N. *J. Chem. Phys.* **1982**, *77*, 2042.

Homogeneous Models for Propylene Ammoxidation. 1. Tungsten(VI) Imido Complexes as Models for the Active Sites

Dominic M.-T. Chan,* William C. Fultz, William A. Nugent, D. Christopher Roe, and Thomas H. Tulip

Contribution No. 3405
Central Research and Development Department
E. I. du Pont de Nemours and Company
Experimental Station, Wilmington, Delaware 19898

Received September 10, 1984

The ammoxidation of propylene is a major industrial process by which eight billion pounds of acrylonitrile are produced annually. In this process, a mixture of propylene, ammonia, and air is passed over a heterogeneous bismuth molybdate catalyst (eq 1). Intense interest in the mechanism of this transformation[1]

$$CH_2{=}CHCH_3 + NH_3 + \frac{3}{2}O_2 \xrightarrow[400\ ^\circ C]{Bi_2O_3/MoO_3} CH_2{=}CHCN + 3H_2O \quad (1)$$

reflects its rather low yield (ca. 65%) when compared with other oxidation reactions (e.g., ca. 90%) for oxidation of propylene to acrolein).

On the basis of studies on heterogeneous systems,[1] the active sites in propylene ammoxidation were proposed[1d] to have structure **1**. At various points in the catalytic cycle, the coordinated group

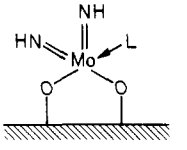

1

(1) For reviews on the mechanism of propylene ammoxidation, see: (a) Keulks, G. W.; Krenzke, L. D.; Notermann, T. M. *Adv. Catal.* **1978**, *27*, 183-225. (b) Haber, J.; Bielanski, A. *Catal. Rev.*—Sci. Eng. **1979**, *19*, 1-41. (c) Gates, B. C.; Katzer, J. R.; Schuitt, G. C. A. "Chemistry of Catalytic Processes"; McGraw-Hill: New York, 1979; pp 325-389. (d) Burrington, J. D.; Kartisek, C. T.; Grasselli, R. K. *J. Catal.* **1983**, *81*, 489-498.

0002-7863/85/1507-0251$01.50/0

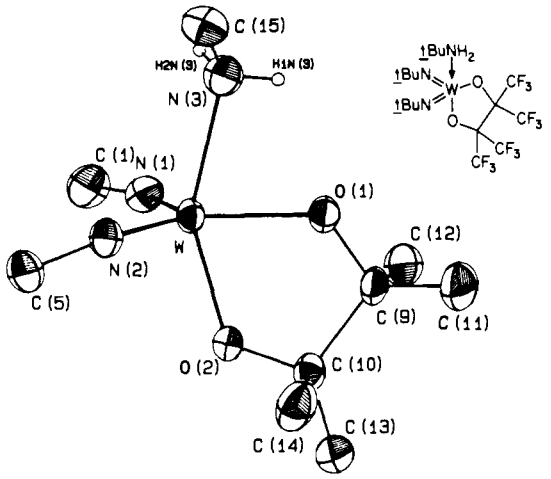

Figure 1. Perspective drawing of (PFP)W(N-*t*-Bu)$_2$(NH$_2$-*t*-Bu) (**4a**) with thermal ellipsoids at the 50% probability level. H atoms are represented by spheres of arbitrary radius. Fluorine atoms and methyl groups are omitted for clarity. Selected distances (Å), W–N(1) = 1.741 (4), W–N(2) = 1.743 (3), W–N(3) = 2.201 (4), and angles, C(1)–N(1)–W = 166.6 (3)°, C(5)–N(2)–W = 164.0 (3)°, C(15)–N(3)–W = 127.4 (3)°.

L in **1** can represent NH_3, H_2O, or the elements of the allyl radical. We wish to report the synthesis and structural characterization of a series of monomeric (pinacolato)tungsten(VI) complexes **5a–c**, which we regard as the first homogeneous models for the imido site **1**.

Perfluoropinacol (**2a**),[2] pinacol (**2b**), and benzopinacol (**2c**) react readily at 25 °C with an equimolar amount of (*t*-BuN)$_2$W(HN-*t*-Bu)$_2$ (**3**)[3] according to eq 2. In each case, ^{1}H and ^{13}C solution

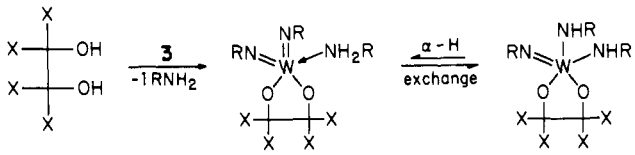

2 **4** **5**

(2)

	X	YIELD	RATIO	
a	CF_3	92%	2.6	1
b	CH_3	100%	1	11
c	Ph	96%	1	20

R = t-Bu

NMR studies indicate the presence of two isomers:[4,5] the aminebis(imido) complex **4** and the imidobis(amido) complex **5**. The ratio of **4**/**5** depends on the glycolate ligand. The more electron-withdrawing perfluoropinacolate (PFP) ligand favors structure **4** while the more electron-donating glycolates reverse this preference. ^{1}H NMR magnetization transfer studies[6] confirm the solution equilibrium between **4a** and **5a** via facile α-hydrogen exchange processes.[7] However, in the solid state, the magic angle spinning ^{13}C NMR spectrum of each product indicates the presence of a single isomer: **4a** in the PFP system and **5b** and **5c** in the pinacolato and benzopinacolato (BZP) complexes.

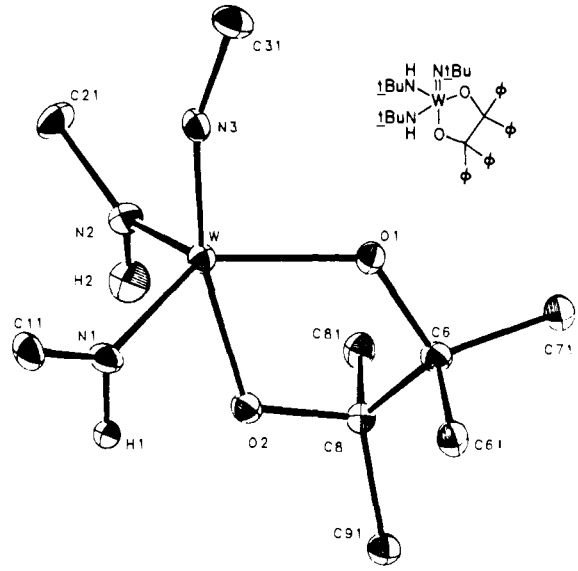

Figure 2. Perspective drawing of (BZP)W(N-*t*-Bu)(HN-*t*-Bu)$_2$ (**5c**) with thermal ellipsoids at the 25% probability level. Methyl groups and part of the aromatic rings are omitted for clarity. Selected distances (Å), W–N(1) = 1.931 (4), W–N(2) = 1.924 (5), W–N(3) = 1.753 (4), and angles, C(11)–N(1)–W = 140.6 (4)°, C(21)–N(2)–W = 139.5 (4)°, C(31)–N(3)–W = 161.0 (4)°.

Single-crystal X-ray diffraction studies confirm our structural assignment for aminebis(imido) **4a**[8,9] (Figure 1) and bis(amido)imido **5c**[10] (Figure 2). Both molecules adopt a distorted trigonal-bipyramidal geometry in which the chelating diol ligand occupies an axial and an equatorial site. The imido groups in both structures are almost linear, indicating significant π-bonding with the metal. The bond distances and angles are in good agreement with other W(VI) imido[11] and PFP[12] complexes. Interestingly, in **4a** the two imido ligands occupy equatorial sites, while in **5c** the imido ligand is axial. In neither complex was there evidence for interaction between the tungsten center and the N–H (amine or amido) hydrogen atoms (average d(W–H) is 2.15 Å in **4a** and 2.37 Å in **5c**).

Several aspects of our results warrant further attention. Replacement of the two η^1-alkoxide groups in (RO)$_2$M(NR)$_2$ by a chelating glycolate ligand clearly increases the tendency of the metal to coordinate a fifth ligand (cf. ref 3). This is pertinent to the recent demonstration that steric coordinative unsaturation of the molybdenum sites play a key role in determining the course of propylene oxidation.[13] The control of equilibrium **4** $\rightleftarrows$ **5** by the electronic nature of the glycolate ligands is relevant to the fundamental question of catalyst–support interactions in ammoxidation. We are actively pursuing both of these aspects. Finally, the successful preparation of *structural* analogues of **1** raises the hope that the *chemistry* of ammoxidation might also be reproduced in solution under mild conditions suitable for mechanistic studies. In the following paper in this series[14] we will demonstrate that this is, in fact, the case.

(2) (a) Middleton, W. J.; Lindsey, R. V. *J. Am. Chem. Soc.* **1964**, *86*, 4948. (b) Astrologes, G. W.; Martin, J. C. *J. Am. Chem. Soc.* **1976**, *98*, 2895.
(3) Nugent, W. A.; Harlow, R. L. *Inorg. Chem.* **1980**, *19*, 777.
(4) Spectroscopic assignments were based on other imido complexes; see ref 5 and: Nugent, W. A.; McKinney, R. J.; Kasowski, R. V.; Van-Catledge, F. A. *Inorg. Chim. Acta* **1982**, *65*, L91. The ratios of isomers **4** and **5** are determined by spectral integration of the ^{1}H NMR *t*-Bu signals.
(5) This is an unexpected result because **3** reacts with 2 equiv of *t*-BuOH to give the well-characterized (*t*-BuN)$_2$W(O-*t*-Bu)$_2$ and 2 equiv of *t*-BuNH$_2$; see ref 3 and: Nugent, W. A. *Inorg. Chem.* **1983**, *22*, 965.
(6) Chan, D. M.-T.; Roe, D. C., unpublished results.
(7) Compare: Rocklage, S. M.; Schrock, R. R.; Churchill, M. R.; Wasserman, H. J. *Organometallics* **1982**, *1*, 1332.
(8) This is the first structurally characterized PFP complex of d^0 transition metal although other high-valent complexes have been prepared: Bramman, P. F.; Lund, T.; Raynor, J. B.; Willis, C. J. *J. Chem. Soc., Dalton Trans.* **1975**, 45. Willis, C. J. *J. Chem. Soc., Chem. Commun.* **1972**, 944.
(9) Structure **4a** refined to R = 0.027 (crystal data in supplementary material).
(10) Structure **5c** refined to R = 0.030 (crystal data in supplementary material).
(11) Thorn, D. L.; Nugent, W. A.; Harlow, R. L. *J. Am. Chem. Soc.* **1981**, *103*, 357. Bradley, D. C.; Errington, R. J.; Hurthouse, M. B.; Nielson, A. J.; Short, R. L. *Polyhedron* **1983**, *2*, 843.
(12) Schomburg, D.; Weferling, N.; Schmutzler, R. *J. Chem. Soc., Chem. Commun.* **1981**, 810. Barnhart, D. M.; Lingafelter, E. C. *Cryst. Struct. Commun.* **1982**, *11*, 733. W-Hague, M.; Ahmed, J.; Horne, W. *Acta. Crystallogr., Sect. C: Cryst. Struct. Commun.* **1983**, *C39*, 1048.
(13) Iwasawa, Y.; Nakamura, T.; Takamatsu, K.; Ogasawara, S. *J. Chem. Soc., Faraday Trans. 1* **1980**, *76*, 939–951. See also: Rappé, A. K.; Goddard, W. A., III. *J. Am. Chem. Soc.* **1982**, *104*, 3827–3294.
(14) Chan, D. M.-T.; Nugent, W. A., manuscript in preparation.

Acknowledgment. We gratefully acknowledge the technical assistance of J. Center and L. Lardear. We also thank Dr. R. D. Farlee for MAS ^{13}C NMR studies and Drs. Y. C. Lin and T. B. Marder for helpful discussions.

Supplementary Material Available: Tables of final positional parameters (as fractional coordinates), thermal parameters, structure factor amplitudes (observed and calculated), and NMR data for the new compounds (34 pages). Ordering information is given on any current masthead page.

Photon-Assisted CH Bond Activation in a Coordinated Methoxy. A Molecular Orbital Explanation

Alfred B. Anderson* and N. K. Ray†

Chemistry Department
Case Western Reserve University
Cleveland, Ohio 44106
Received July 13, 1984

Methoxy groups can be formed on unsaturated Mo^{VI} centers on edge surfaces of layered-structure MoO_3[1] and found on the surface of the $Mo_8O_{24}(OCH_3)_4^{4-}$ anion.[2] Thermally activated dehydrogenation occurs on warming MoO_3 to 217 °C, and at 500 °C for the anion, yielding formaldehyde and water. Exposure of the anion to UV light causes formaldehyde to form from the anion under ambient conditions, and similar behavior is seen for $Mo_2O_5(OCH_3)_2$.[3] The purpose of this paper is to explain the photoactivation of methoxy CH bonds in these systems by using molecular orbital theory.

There are sufficient similarities between the anion[2] and bulk MoO_3[4] structures (layering of distorted octahedra) to allow the use of a MoO_3 bulk-superimposable $Mo_3O_{13}^{8-}$ model with methoxy coordinated as in Figure 1. Atom superposition and electron delocalization molecular orbital (ASED-MO) theory parameters for Mo and O come from an earlier study[5] of the electronic properties of crystalline MoO_3. For C, the respective 2s and 2p orbital exponents and ionization potentials are 1.65 au, 18 eV, and 1.618 au, 9.26 eV; for H, the 1s parameters are 1.2 au and 11.6 eV. In the ASED-MO theory the electronic charge density of a molecule is partitioned into free-atom parts and an electron delocalization bond formation component. As the atoms bond together forming a molecule, the electrostatic forces on the nuclei are integrated to yield a repulsive energy due to rigid-atom densities and an attractive energy due to electron delocalization. The sum is the exact molecular binding energy. The atom superposition energy is easily calculated and the electron delocalization energy, though not directly calculable, is well approximated by a one-electron molecular orbital energy obtained by using a hamiltonian which shares some features with the extended Hückel hamiltonian. Our truncated model produces the electronic structure in Figure 2. All of the bands widen somewhat for larger clusters. The electronic structure of a $Mo_6O_{25}^{14-}$ cluster shown in ref 5 is more representative in this regard of the anion being modeled here and of a $Mo_6O_{19}^{3-}$ anion.[6] By comparison of the calculated electronic structure of $Mo_6O_{25}^{14-}$ with the optical spectrum of $Mo_6O_{13}^{3-}$, it is evident that the observed[6] transitions at 11 600 and 20 400 cm^{-1} are due to d-d transitions within the lower and between the lower and middle bands, respectively. The

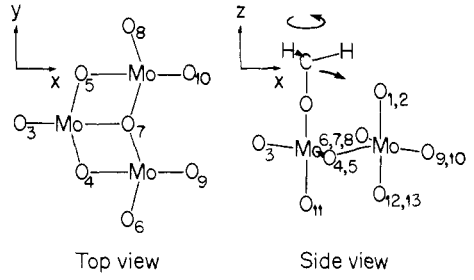

Figure 1. $Mo_3O_{13}OCH_3^{9-}$ structure.

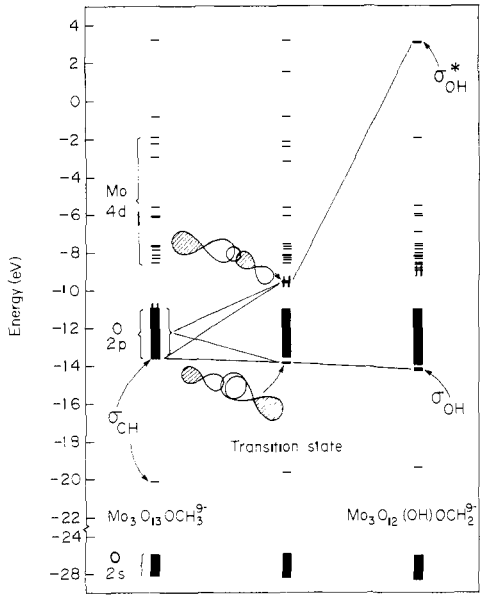

Figure 2. Orbital energy level correlations during the course of methoxy dehydrogenation to form formaldehyde and hydroxide

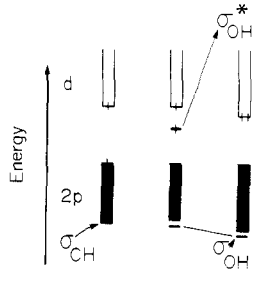

Figure 3. As in Figure 2 showing electron occupations for the reaction on the cluster with an electron–hole pair excitation.

strong transition at ~31 000 cm^{-1} is due to O 2p to Mo 4d charge transfer. In $Mo_8O_{24}(OCH_3)_4$ the 4d bands are empty and this charge-transfer excitation is expected to be active toward the dehydrogenation of coordinated methoxy.

When the methoxy group is rotated and tilted so that the Mo–O–C angle is 160°, the CH bond may be stretched to a transition state with CH and OH distances of 1.85 and 1.30 Å, respectively, and an H–O_1–Mo angle of 158°. The important stabilization at the transition state is a three-center C–H–O σ bond (Figure 2). The CH–O antibonding orbital is also doubly occupied, giving rise to the energy level in the O 2p–Mo 4d band gap shown in Figure 2. This orbital becomes the empty high-lying OH σ^*, and the cluster is reduced by two electrons. The calculated activation energy is 2.6 eV, which is approximate because of the nature of the theory, the structure model, and the omission of cluster geometry relaxations in the transition state.

The transition-state geometry is nearly the same when an electron is promoted from the top of the O 2p band to the bottom of the Mo 4d band. The activation energy, however, is reduced by nearly half to 1.4 eV. As may be seen in Figure 3, *the photoactivation is a consequence of transferring the electron hole to*

† On leave from the Department of Chemistry, University of Delhi, Delhi 7, India.

(1) Chowdhry, V.; Ferretti, A.; Firment, L. E.; Machiels, C. J.; Ohuchi, F.; Sleight, A. W.; Staley, R. H. *Appl. Surf. Sci.*, in press.
(2) McCarron, E. M., III; Harlow, R. L., I. *J. Am. Chem. Soc.* **1983**, *105*, 6179.
(3) McCarron, E. M., III; Staley, R. H.; Sleight, A. W. *Inorg. Chem.* **1984**, *23*, 1043.
(4) Wyckoff, R. W. G. "Crystal Structures", 2nd ed.; Wiley: New York, 1964; Vol. 2.
(5) Anderson, A. B.; Kim, Y.; Ewing, D. W.; Grasselli, R. K.; Tenhover, M. *Surf. Sci.* **1983**, *134*, 237.
(6) Sanchez, C.; Livage, J.; Launay, J. P.; Fournier, M.; Jeannin, Y. *J. Am. Chem. Soc.* **1982**, *104*, 3194.

0002-7863/85/1507-0253$01.50/0